Molecular Rotors

International Edition: DOI: 10.1002/anie.201712381
German Edition: DOI: 10.1002/ange.201712381

Dynamic Ultralong Organic Phosphorescence by Photoactivation

Long Gu[+], Huifang Shi[+], Mingxing Gu[+], Kun Ling, Huili Ma, Suzhi Cai, Lulu Song, Chaoqun Ma, Hai Li, Guichuan Xing, Xiaochun Hang, Jiewei Li, Yaru Gao, Wei Yao, Zhigang Shuai, Zhongfu An, Xiaogang Liu,* and Wei Huang**

Abstract: *Smart materials with ultralong phosphorescence are rarely investigated and reported. Herein we report on a series of molecules with unique dynamic ultralong organic phosphorescence (UOP) features, enabled by manipulating intermolecular interactions through UV light irradiation. Our experimental data reveal that prolonged irradiation of single-component organic phosphors of PCzT, BCzT, and FCzT under ambient conditions can activate UOP with emission lifetimes spanning from 1.8 to 1330 ms. These phosphors can also be deactivated back to their original states with short-lived phosphorescence by UV irradiation for 3 h at room temperature or through thermal treatment. Additionally, the dynamic UOP was applied successfully for a visual anti-counterfeiting application. These findings may provide unique insight into dynamic molecular motion for optical processing and expand the scope of smart-response materials for broader applications.*

Smart-response materials whose physical properties, such as spin transitions,[1] charge transfer,[2] and ground or excited state,[3] as well as structural changes, can be tuned controllably by external stimuli, including light,[4] humidity,[5] pressure,[6] and magnetic or electric fields,[7,8] play critical roles in diverse fields, such as information storage and encryption,[9] molecular machines,[10–12] biomedicine,[13] and electroconductibility.[14] The dynamic features of these materials endow optoelectronic devices with revolutionary performance. For example, through photoinduced molecular structure changes, molecular materials may have dynamic bistable states for reversible switching or optical memory.[14,15] Molecular motors or actuators can be constructed by the conversion of an external stimulus into mechanical actuation.[16] Under an electric field, a data-recording device was fabricated on the basis of a smart-response phosphorescence material.[17] Despite great progress in realizing dynamic control over the variation of photophysical properties, there are still large barriers to the development of an advanced system with dynamic behavior modulated by external stimuli.

Ultralong phosphorescence with a long-lived excited state, that is, persistent luminescence, has received considerable attention owing to its fundamental scientific importance and potential technological applications, ranging from display and emergency signage to document security and bioimaging,[18–20] which has been limited to inorganic materials. Intrinsic obstacles to the use of inorganic phosphors, such as harsh preparation conditions, scarcity of metal resource components, and high toxicity for bioapplications, have led to many alternate and effective approaches, such as host–guest doping, crystallization, and H-aggregation.[21–24] These approaches were recently investigated to generate ultralong phosphorescence in metal-free organics at room temperature. Such ultralong phosphorescence shows steady-state optical behavior.[25] To the best of our knowledge, researchers have yet to find a molecular system capable of dynamic ultralong phosphorescence. Inspired by the rational manipulation of molecular stacking by alkyl-chain engineering[26] and dynamic motion in crystalline molecule machines,[27] we speculate herein that dynamic organic phosphorescence might be induced by harvesting the synergistic effects of intermolecular interactions and molecular motion within a new class of molecular rotors resting in the crystalline state. By means of photoirradiation in the crystalline state to manipulate intermolecular interactions, dynamic optical behavior may be realized to stabilize triplet excitons for ultralong phosphorescence through molecular motion.

To validate our hypothesis, we designed and prepared a series of molecular rotors containing a triazine core, a carbazole unit, and alkoxy chains (Figure 1 a). The chromophore composed of a carbazole and a triazine unit serves as a rotor to drive the molecular motion for manipulating intermolecular interactions through photoirradiation, thus suppressing nonradiative transition to stabilize excited triplet excitons for ultralong organic phosphorescence (UOP). The introduction of alkoxy chains can fine-tune the molecular arrangement and displacement, but has little influence on the excited-state properties in the single-molecule state. As the

[*] L. Gu,[+] Dr. H. Shi,[+] M. Gu,[+] K. Ling, Dr. H. Ma, S. Cai, L. Song, C. Ma, Prof. H. Li, Prof. G. Xing, Prof. X. Hang, Dr. J. Li, Y. Gao, Dr. W. Yao, Prof. Z. An, Prof. W. Huang
Key Laboratory of Flexible Electronics (KLOFE) and Institute of Advanced Materials (IAM), Nanjing Tech University (NanjingTech)
30 South Puzhu Road, Nanjing 211800 (China)
E-mail: iamzfan@njtech.edu.cn
iamwhuang@njtech.edu.cn
Prof. W. Huang
Shaanxi Institute of Flexible Electronics (SIFE)
Northwestern Polytechnical University (NPU)
127 West Youyi Road, Xi'an 710072 (China)
Prof. X. Liu
Department of Chemistry, National University of Singapore
Singapore 117543 (Singapore)
E-mail: chmlx@nus.edu.sg
Prof. Z. Shuai
Key Laboratory of Organic OptoElectronics and Molecular Engineering, Department of Chemistry, Tsinghua University
Beijing 100084 (P. R. China)
[+] These authors contributed equally.
Supporting information and the ORCID identification number(s) for the author(s) of this article can be found under: https://doi.org/10.1002/anie.201712381.

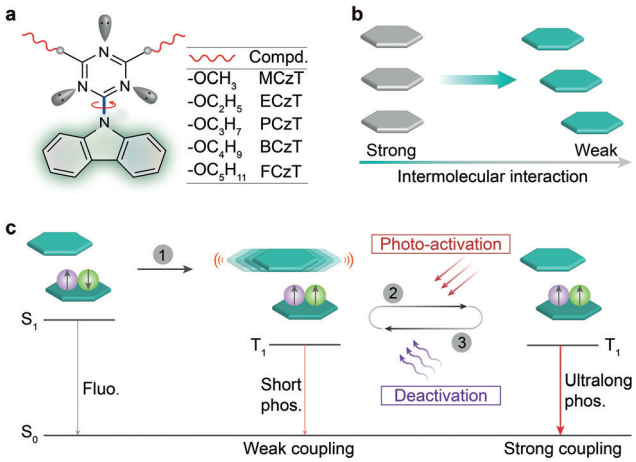

Figure 1. a) Rational design of molecular rotors. b) Molecular packing modes in crystals. c) Proposed mechanism for dynamic ultralong organic phosphorescence.

length of the alkoxy chains increased from methoxy to *n*-pentoxy, molecular configurations exhibited a twisting angle for single molecules in the crystal. The packing modes show a relative stepped arrangement from MCzT to FCzT (Figure 1b). Importantly, a unique phenomenon of dynamic UOP was realized by prolonged irradiation to drive molecular motion. As shown in Figure 1c, the triplet excitons are generated from the singlet excitons through intersystem crossing (step 1), enabling short-lifetime phosphorescence owing to boosted nonradiative transition. After the molecules in the crystal are photoactivated by prolonged irradiation with a UV lamp (step 2) and then thermally deactivated (step 3), the intermolecular interaction varies in the distance between neighboring molecules as a result of molecular motion, which should provide a possibility to rationally tune nonradiative transitions for stabilization of the triplet excitons, thus making reversible UOP possible.

In the solid state, the compounds under study exhibited similar blue emission bands around 370 and 385 nm with fine vibrational structures (Figure 2a, left). However, with longer alkoxy groups and under ambient conditions, completely different phosphorescent behavior could be visualized by the naked eye after switching off the UV lamp. Both MCzT and ECzT showed UOP that lasted for several seconds after irradiation with a 365 nm UV lamp (see the Supporting

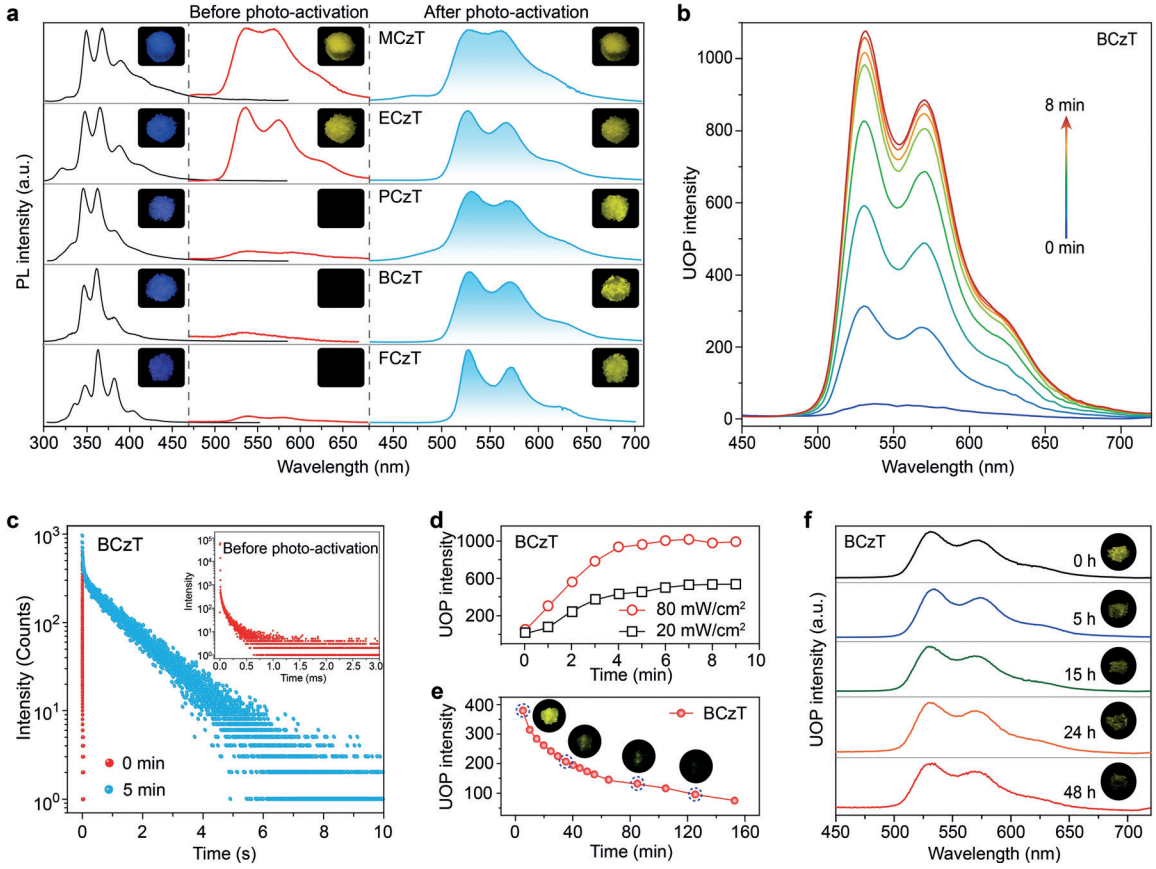

Figure 2. a) Steady-state photoluminescence (black line) and phosphorescence spectra of the phosphors before (red line) and after photoactivation (blue line) under ambient conditions. Photographs of the corresponding phosphors before and after photoactivation are also shown. b) Phosphorescence spectra of BCzT crystals after different photoactivation times ranging from 0 to 8 min under ambient conditions. c) Lifetime decay profiles of the emission band around 530 nm of BCzT crystals before and after photoactivation under ambient conditions. The inset shows an enlarged view of the lifetime decay profile of BCzT crystals before photoactivation. d) UOP intensity of BCzT in the crystal at 530 nm with varying photoactivation times and different powers of the irradiation light source under ambient conditions. e) Deactivation process of the UOP for BCzT after continuous UV irradiation for 5 min under ambient conditions. f) UOP spectra of photoactivated BCzT crystals after being kept in liquid nitrogen for different times ranging from 0 to 48 h. Note that BCzT crystals were first photoactivated for 5 min by a 365 nm lamp. Corresponding ultralong phosphorescence photographs of BCzT crystals after flash photoirradiation under ambient conditions are also shown.

Information, videos SV1 and SV2). In contrast, for the compounds PCzT, BCzT, and FCzT, no visible luminescence was noticeable; however, weak phosphorescence signals were detected by a sensitive PL spectrometer (Figure 2a, middle). Surprisingly, we observed bright, ultralong luminescence with durations of several seconds for PCzT, BCzT, and FCzT when irradiated continuously by a UV lamp for less than 10 min (see SV3–SV5). Herein, the prolonged irradiation is defined as a photoactivation process. Furthermore, with increasing chain length of the alkoxy group, the phosphorescence efficiency of these luminogens gradually decreased from 2.5 to 0.8% (see Table S1 in the Supporting Information).

To understand the nature of this UOP feature, we conducted a further set of experiments on BCzT as a model system. As the photoactivation time was increased from 0 to 8 min, the phosphorescence intensity of BCzT in the crystalline state was enhanced by a factor of 30, along with receding fluorescence intensity (Figure 2b; see also Figure S12b in the Supporting Information). Meanwhile, the lifetime of emission at 530 nm showed a sharp increase from 1.8 to 1330 ms after BCzT was photoactivated for 10 min with a UV lamp under ambient conditions (Figure 2c). The photoactivation process could also be observed under a high vacuum, under nitrogen, and under oxygen at room temperature (see Figures S13–S15). The long-lived emission of the BCzT crystal remained after irradiation for 5 min with a UV lamp, thus indicating that the photoactivation phenomenon is independent of the environment. Furthermore, we further investigated the effect of excitation intensity on photoactivation time for BCzT. As the excitation light intensity was increased from 20 to 80 mW cm^{-2}, the photoactivation time shortened gradually (Figure 2d).

Significantly, the photoactivated UOP disappeared gradually when BCzT crystals were kept either under ambient conditions or under vacuum at room temperature for about 160 min (Figure 2e; see Figure S17 and video SV6), thus suggesting the occurrence of a dynamic process. When photoactivated crystals were kept in liquid nitrogen at 77 K, UOP could still be observed by the naked eye after 48 h, as the deactivation process was slowed down (Figure 2f; see also Figure S18). In contrast, photoactivated BCzT was deactivated to its original state when heated at 338 K for 5 min (see Figure S29b). Taken together, these results suggest that the deactivation process of photoactivated BCzT crystals is thermally controlled. Notably, the reversibility of dynamic UOP was further confirmed through repeated cycles of photoactivation and deactivation at room temperature (see Figure S30).

To probe the mechanism underlying this unique dynamic UOP, a set of control experiments, theoretical calculations, and single-crystal structure analyses were carried out before and after photoactivation. As the duration of photoactivation was prolonged at room temperature, we observed an increase in the phosphorescence lifetime of the BCzT crystal (Figure 3a). This result is consistent with the gradual increase observed in the phosphorescence lifetime as the temperature was decreased from room temperature to 77 K (Figure 3b). Impressively, it was not until around 233 K that UOP could be observed after irradiation with a 365 nm hand-held UV lamp (see Figure S32). Given that the prolonged lifetimes are likely to be due to suppression of a nonradiative transition caused by molecular vibrations under frozen conditions,[28] we speculate that the photoactivation might play a similar role to the freezing process. In the crystal, the simulation shows that the nonradiative transition mainly stems from breathing vibrations of carbazole groups along the planar direction (see Figure S36 and GIF in the Supporting Information), which might be the cause of dynamic UOP. As anticipated, the distances of intermolecular interactions between two adjacent molecules after photoactivation in the same plane indeed decreased as compared with those before photoactivation, from 2.661 and 2.702 Å to 2.635 and 2.677 Å between carbazole and triazine groups, and from 2.382 and 2.853 Å to 2.351 and 2.833 Å between carbazole and butoxy units, and from 2.343 to 2.293 Å between butoxy substituents in adjacent planes (Figure 3c). The resulting much stronger intermolecular interactions limit the nonradiative transition, as required for ultralong phosphorescence, by stabilizing the triplet excitons. Additionally, one more intermolecular interaction appeared within a distance of 2.380 Å between carbazole and butoxy units after photoactivation. Thus, it is suggested that restriction of the nonradiative transition caused by adjacent molecular vibrations may be the main reason for the dynamic UOP observed in the crystal.

In the BCzT crystal, two identical alkoxy chains connected by a triazine center display quite different conformations (see Figure S38), resulting in dihedral angles of 5.68 and 5.58° between the triazine and carbazole planes. After photoactivation, the dihedral angles between the two planes changed to 5.24 and 5.92° along with variation in bond length (see Figure S37b and Tables S9 and S10), thus indicating that photoirradiation enables molecular motion to controllably tune nonradiative transitions in the crystal. The molecular motions were further confirmed by atomic force microscopy (AFM). Before photoactivation, the BCzT crystal adopted an almost uniform layered surface topography (Figure 3d, top). However, the surface of the same crystal displayed undulations after photoactivation for 5 min (Figure 3d, bottom). Upon storage for 2 days under ambient conditions, the uniform layered surface topography of the crystal was recovered (see Figure S39).

To further illustrate the role of UV light in tuning intermolecular interactions for dynamic UOP in the crystals, we carried out a set of control experiments. No photoactivated ultralong organic phosphorescence (UOP) was observed after the irradiation wavelength was changed from 365 nm (UV light) to 450 or 500 nm (see Figure S40a and video SV7). It was found that the BCzT crystal showed strong absorption in the ultraviolet region (see Figure S40b). In other words, the BCzT molecule can be excited by UV light to generate excited states. During the transition of the BCzT molecule from the ground state to the excited state, we observed a change in the molecular configuration, which was further confirmed by theoretical simulations (see Figure S34). In the gas state, there existed a large molecular structure transformation from the ground state to the excited state owing to free intermolecular interactions. In the solid state, owing to the strong suppression of intermolecular interac-

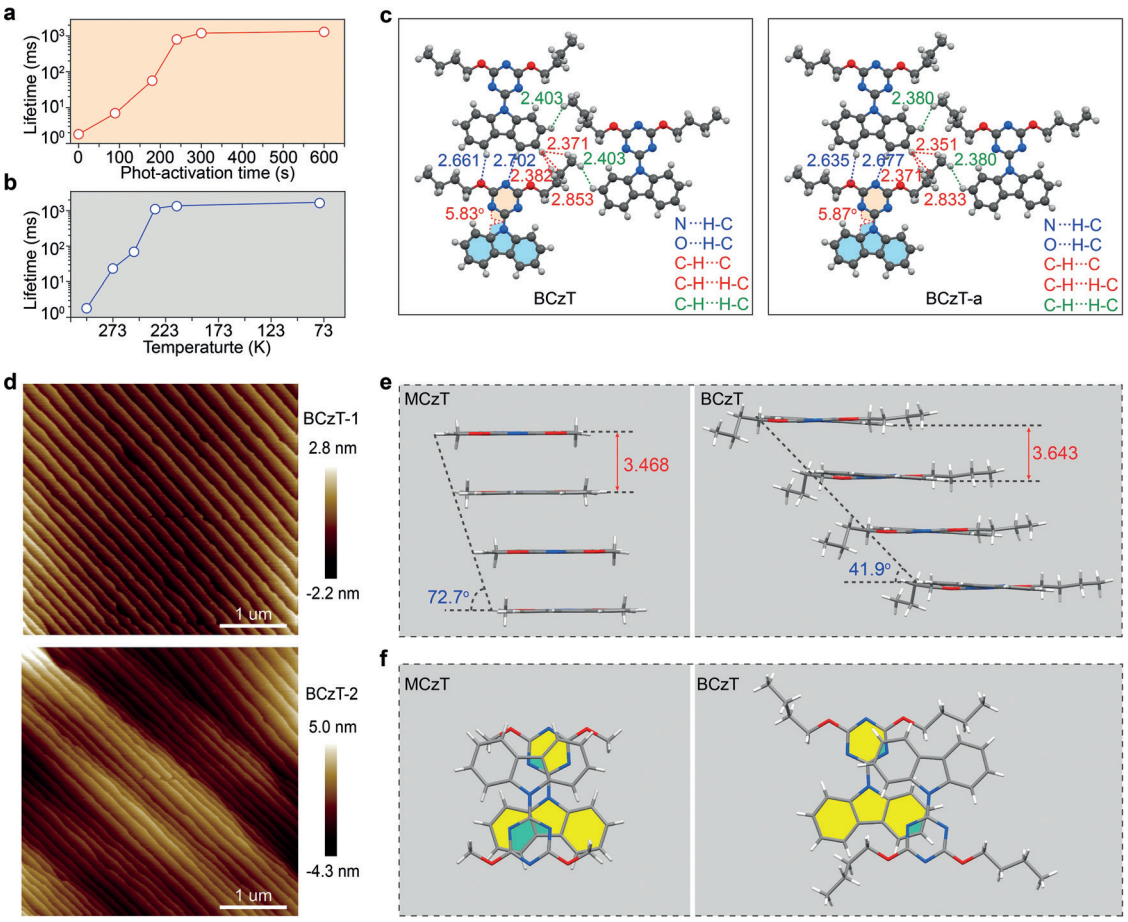

Figure 3. a) Lifetime tendency of the BCzT crystal at 530 nm emission with different photoactivation durations under ambient conditions. b) Lifetime tendency of the BCzT crystal at 530 nm emission at different temperatures (298, 273, 253, 233, 213, and 77 K). c) Intermolecular interactions and twisting angles of BCzT in a single crystal before and after photoactivation (BCzT-a) at 100 K. d) AFM topographic images of a BCzT crystal recorded before (above) and after (below) photoactivation by UV irradiation for 5 min under ambient conditions. e, f) Side and top views, respectively, of the molecular packing modes of MCzT and BCzT.

tions, the variation of molecular configuration was relatively small, which is consistent with the change in molecular configuration before and after photoactivation by UV light. From these results, we reason that UV light plays a critical role in controlling molecular configuration and tuning intermolecular interactions in the crystal. Additionally, it was found that the ground-state energy after photoactivation was 0.153 eV higher than that before photoactivation (see Figure S42), thus indicating that there existed a higher-energy and metastable ground state for tuning the deactivation of dynamic UOP.

To gain deeper insight into the molecular motion in a crystal, we studied the single-crystal structure of MCzT with inherent UOP as a control experiment. BCzT displays a lower slip angle between π-stacked molecules of 41.88° as compared to MCzT (72.65; Figure 3e), thus resulting in less molecular overlap between neighboring molecules (Figure 3f). Therefore, the intermolecular interaction was weakened, favoring the possibility of molecular motion. It is speculated that the partial interaction between adjacent π-stacked molecules plays a vital role in regulating photoinduced molecular motion, as required to tune nonradiative transitions and enable dynamic UOP.

To validate our hypothesis, the single-crystal structures of PCzT and FCzT were investigated. Reduced intermolecular overlap was also observed in PCzT and FCzT crystals (see Figures S44 and S45). As for BCzT, dynamic UOP was also observed as anticipated in PCzT and FCzT after photoactivation for 7 and 1 min, respectively. As shown in Figure 4a,b, the photoactivation and deactivation times of dynamic UOP were in inverse proportion to the alkoxy chain lengths of these phosphors. As the length of the alkoxy chain increased, the lifetime of both photoactivation and deactivation for UOP decreased drastically from 4.77 to 0.99 min and 119 to 18 min (see Figure S46 and Table S11), respectively. Furthermore, besides triazine derivatives, the generality of our approach for the generation of dynamic UOP was further approved in a crystal of a pyridine derivative (PyCz). Similar dynamic UOP behavior to that of BCzT was observed in the crystal (see Figure S47 and video SV8). After photoactivation, bright ultralong phosphorescence with a lifetime of 776.03 ms was observed. By single-

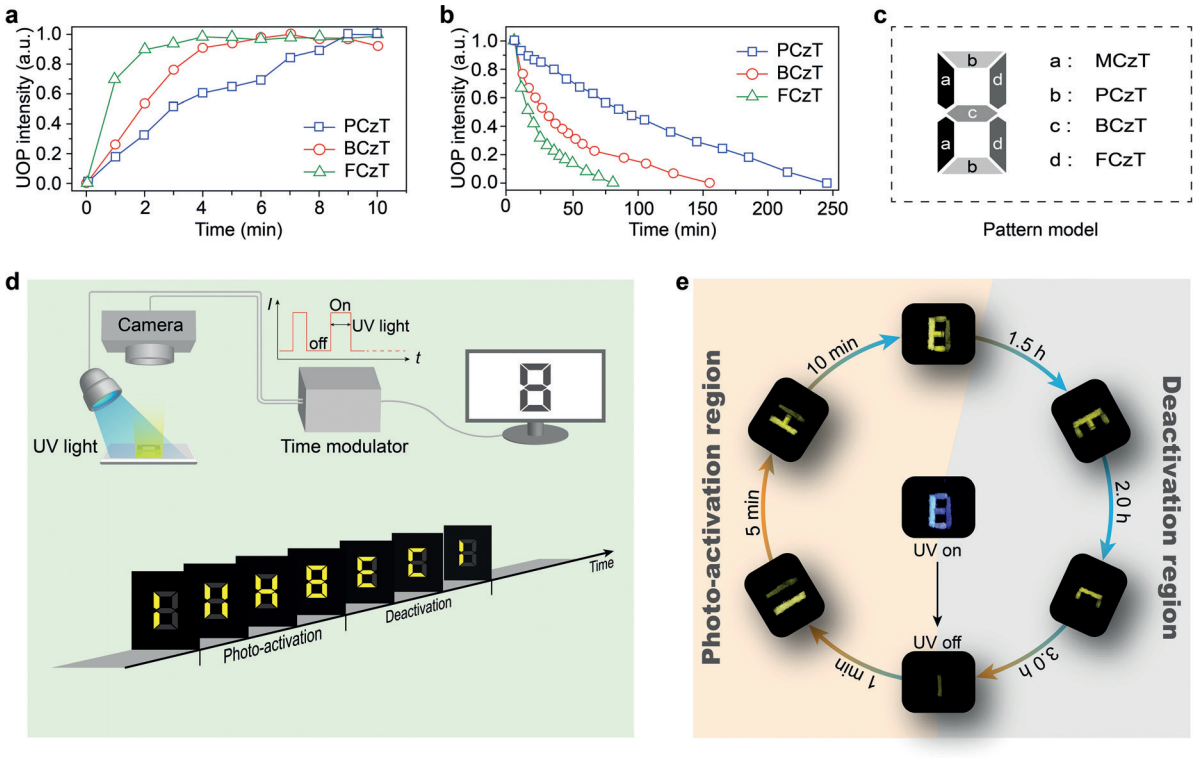

Figure 4. a) Intensity of 530 nm UOP of PCzT, BCzT, and FCzT crystals as a function of photoactivation time from 0 to 10 min under ambient conditions. Irradiation power: 80 mW cm^{-2}. b) UOP deactivation process: Monitoring of the emission intensities of PCzT, BCzT, and FCzT crystals at 530 nm under ambient conditions. c) Pattern designed with different phosphors. d) Experimental setup for the multilevel anti-counterfeiting device. By modulating the photoactivation and deactivation times, different digits and letters can be captured by the naked eye. e) Demonstration of multilevel anti-counterfeiting using the MCzT, PCzT, BCzT, and FCzT crystals.

crystal analysis, it was found that more intermolecular interactions appeared after the sample was photoactivated by UV light (see Figure S47 d), thus leading to much stronger intermolecular interactions to suppress nonradiative transitions. As for BCzT, molecular overlap between neighboring molecules was small (see Figure S47 e).

Given the unique dynamic UOP features of MCzT, PCzT, BCzT, and FCzT with various photoactivation and deactivation times, an anti-counterfeiting pattern "8" was fabricated using different phosphors (Figure 4 c). The results of photoactivation and deactivation are shown in Figure 4 d. Under 365 nm UV-lamp irradiation, the pattern displayed a digital number "8". When the UV-lamp exposure was interrupted before photoactivation, a visible letter "I" was visible to the naked eye due to the inherent UOP of MCzT. Furthermore, when UV-lamp exposure was interrupted after photoactivation for 1 min, the luminescent pattern changed to the digital number "11" because the UOP of FCzT can be generated within 1 min of photoactivation. Similarly, the luminescent pattern could be converted into the letter "H" and finally to the full digital number "8" by means of different photoactivation times of 5 and 10 min for BCzT and PCzT crystals, respectively. Thus, quadruple data encryption and decryption have been realized by this photoactivated dynamic UOP process. Subsequently, a deactivation process of this unique dynamic UOP occurred. After delays of 1.5, 2.5, and 3.5 h, the decrypted digit "8" was further encrypted to the letters "E" and "C", and returned to "I", respectively. Importantly, this special dynamic UOP characteristic enables reversible, multilevel data encryption and decryption as well as high-density data storage, a dynamic process that is inaccessible by conventional approaches.

In conclusion, we have developed a series of molecular rotors for dynamic and reversible ultralong organic phosphorescence by manipulating intermolecular interactions in the crystalline state with external stimuli. Upon prolonged photoirradiation, the UOP of these crystalline materials could be activated, resulting in sharply increased emission lifetimes under ambient conditions from several milliseconds to seconds: a broad range of values covering nearly three orders of magnitude. These phosphors were deactivated to their original states of short-lived phosphorescence over time or through thermal treatment. By tailoring the alkoxy chains in these molecular rotors, dynamic UOP behavior with different photoactivation and deactivation times could be controllably tuned under ambient conditions, as evidenced by a visual, multilevel anti-counterfeiting demonstration. This study not only upends conventional notions about organic phosphorescence, but also offers a novel platform for the development of versatile smart materials with precisely tunable characteristics to revolutionize the fields of molecular

machines, information encryption, and security as well as organic optoelectronics.

Acknowledgements

This study was supported by the National Natural Science Foundation of China (51673095 and 61505078), the National Basic Research Program of China (973 Program, No. 2015CB932200), the Natural Science Foundation (BK20150962), the Natural Science Fund for Colleges and Universities (17KJB430020) in Jiangsu Province, the National Research Foundation, Prime Minister's Office, Singapore under its Competitive Research Program (CRP Award No. NRF-CRP15-2015-03), "High-Level Talents in Six Industries" (XCL-025) of Jiangsu Province, and NanjingTech Start-up Grant (3983500158 and 3983500169).

Conflict of interest

The authors declare no conflict of interest.

Keywords: crystal engineering · dynamic ultralong phosphorescence · multilevel anti-counterfeiting · photoactivation · photophysics

How to cite: *Angew. Chem. Int. Ed.* **2018**, *57*, 8425 – 8431
Angew. Chem. **2018**, *130*, 8561 – 8567

[1] S. Ohkoshi, K. Imoto, Y. Tsunobuchi, S. Takano, H. Tokoro, *Nat. Chem.* **2011**, *3*, 564 – 569.
[2] T. Miyamoto, H. Yada, H. Yamakawa, H. Okamoto, *Nat. Commun.* **2013**, *4*, 3586 – 3595.
[3] M. Irie, T. Fukaminato, K. Matsuda, S. Kobatake, *Chem. Rev.* **2014**, *114*, 12174 – 12277.
[4] S. Kobatake, S. Takami, H. Muto, T. Ishikawa, M. Irie, *Nature* **2007**, *446*, 778 – 781.
[5] H. Arazoe, D. Miyajima, K. Akaike, F. Araoka, E. Sato, T. Hikima, M. Kawamoto, T. Aida, *Nat. Mater.* **2016**, *15*, 1084 – 1089.
[6] K. Lekin, H. Phan, S. Winter, J. L. Wong, P. A. Dube, M. Shatruk, R. Oakley, *J. Am. Chem. Soc.* **2014**, *136*, 8050 – 8062.
[7] O. Sato, *Nat. Chem.* **2016**, *8*, 644 – 656.
[8] N. Ozaki, H. Sakamoto, T. Nishihara, T. Fujimori, Y. Hijikata, R. Kimura, S. Irle, K. Itami, *Angew. Chem. Int. Ed.* **2017**, *56*, 11196 – 11202; *Angew. Chem.* **2017**, *129*, 11348 – 11354.
[9] O. Kahn, C. Jay Martinez, *Science* **1998**, *279*, 44 – 48.
[10] W. R. Browne, B. L. Feringa, *Nat. Nanotechnol.* **2006**, *1*, 25 – 35.
[11] B. Champin, P. Mobian, J. Sauvage, *Chem. Soc. Rev.* **2007**, *36*, 358 – 366.
[12] C. Pezzato, C. Cheng, J. F. Stoddart, R. D. Astumian, *Chem. Soc. Rev.* **2017**, *46*, 5491 – 5507.
[13] K. Kinbara, T. Aida, *Chem. Rev.* **2005**, *105*, 1377 – 1400.
[14] a) C. Jia, A. Migliore, N. Xin, S. Huang, J. Wang, Q. Yang, S. Wang, H. Chen, D. Wang, B. Feng, Z. Liu, G. Zhang, D. Qu, H. Tian, M. Ratner, H. Xu, A. Nitzan, X. Guo, *Science* **2016**, *352*, 1443 – 1445.
[15] a) T. Leydecker, M. Herder, E. Avlica, G. Bratina, S. Hecht, A. Orgiu, P. Samorì, *Nat. Nanotechnol.* **2016**, *11*, 769 – 775; b) Z. Liang, T.-H. Tsoi, C.-F. Chan, L. Dai, Y. Wu, G. Du, L. Zhu, C.-S. Lee, W.-T. Wong, G.-L. Law, K.-L. Wong, *Chem. Sci.* **2016**, *7*, 2151 – 2156.
[16] J. Foy, Q. Li, A. Goujon, Je. Colard-Itté, G. Fuks, E. Moulin, O. Schiffmann, D. Dattler, D. Funeriu, N. Giuseppone, *Nat. Nanotechnol.* **2017**, *12*, 540 – 545.
[17] H. Sun, S. Liu, W. Lin, K. Zhang, W. Lv, X. Huang, F. Huo, H. Yang, G. Jenkins, Q. Zhao, W. Huang, *Nat. Commun.* **2014**, *5*, 3601 – 3609.
[18] Z. Pan, Y. Lu, F. Liu, *Nat. Mater.* **2012**, *11*, 58 – 63.
[19] K. Jiang, L. Zhang, J. Lu, C. Xu, C. Cai, H. Li, *Angew. Chem. Int. Ed.* **2016**, *55*, 7231 – 7235; *Angew. Chem.* **2016**, *128*, 7347 – 7351.
[20] T. Maldiney, A. Bessière, J. Seguin, E. Teston, S. Sharma, B. Viana, A. Bos, P. Dorenbos, M. Bessodes, D. Gourier, D. Scherman, C. Richard, *Nat. Mater.* **2014**, *13*, 418 – 426.
[21] a) S. Hirata, K. Totani, J. Zhang, T. Yamashita, H. Kaji, S. Marder, T. Watanabe, C. Adachi, *Adv. Funct. Mater.* **2013**, *23*, 3386 – 3397; b) Y. Katsurada, S. Hirata, K. Totani, T. Watanabe, M. Vacha, *Adv. Opt. Mater.* **2015**, *3*, 1726 – 1737.
[22] a) Y. Xie, Y. Ge, Q. Peng, C. Li, Q. Li, Z. Li, *Adv. Mater.* **2017**, *29*, 1606829 – 1606836; b) M. Shimizu, R. Shigitani, M. Nakatani, K. Kuwabara, Y. Miyake, K. Tajima, H. Sakai, T. Hasobe, *J. Phys. Chem. C* **2016**, *120*, 11631 – 11639; c) Z. Yang, Z. Mao, X. Zhang, D. Ou, Y. Mu, Y. Zhang, C. Zhao, S. Liu, Z. Chi, J. Xu, Y. Wu, A. Lien, M. Bryce, *Angew. Chem. Int. Ed.* **2016**, *55*, 2181 – 2185; *Angew. Chem.* **2016**, *128*, 2221 – 2225; d) Y. Gong, G. Chen, Q. Peng, W. Yuan, Y. Xie, S. Li, Y. Zhang, B. Tang, *Adv. Mater.* **2015**, *27*, 6195 – 6201; e) Y. Shoji, Y. Ikabata, Q. Wang, D. Nemoto, A. Sakamoto, N. Tanaka, J. Seino, H. Nakai, T. Fukushima, *J. Am. Chem. Soc.* **2017**, *139*, 2728 – 2733; f) Y. Gong, L. Zhao, Q. Peng, D. Fan, W. Yuan, Y. Zhang, B. Tang, *Chem. Sci.* **2015**, *6*, 4438 – 4444; g) J. Wei, B. Liang, R. Duan, Z. Cheng, C. Li, T. Zhou, Y. Yi, Y. Wang, *Angew. Chem. Int. Ed.* **2016**, *55*, 15589 – 15593; *Angew. Chem.* **2016**, *128*, 15818 – 15822; h) Z. Chai, C. Wang, J. Wang, F. Liu, Y. Xie, Y. Zhang, J. Li, Q. Li, Z. Li, *Chem. Sci.* **2017**, *8*, 8336 – 8344; i) L. Xiao, Y. Wu, Z. Yu, Z. Xu, J. Li, Y. Liu, J. Yao, H. Fu, *Chem. Eur. J.* **2018**, *24*, 1801 – 1805.
[23] a) Z. An, C. Zheng, Y. Tao, R. Chen, H. Shi, T. Chen, Z. Wang, H. Li, R. Deng, X. Liu, W. Huang, *Nat. Mater.* **2015**, *14*, 685 – 690; b) S. Cai, H. Shi, J. Li, L. Gu, Y. Ni, Z. Cheng, S. Wang, W. Xiong, L. Li, Z. An, *Adv. Mater.* **2017**, *29*, 1701244 – 1701250; c) E. Lucenti, A. Forni, C. Botta, L. Carlucci, C. Giannini, D. Marinotto, A. Pavanello, A. Previtali, S. Righetto, E. Cariati, *Angew. Chem. Int. Ed.* **2017**, *56*, 16302 – 16307; *Angew. Chem.* **2017**, *129*, 16520 – 16525; d) E. Lucenti, A. Forni, C. Botta, L. Carlucci, C. Giannini, D. Marinotto, A. Previtali, S. Righetto, E. Cariati, *J. Phys. Chem. Lett.* **2017**, *8*, 1894 – 1898.
[24] a) G. Zhang, J. Chen, S. J. Payne, S. E. Kooi, J. N. Demas, C. L. Fraser, *J. Am. Chem. Soc.* **2007**, *129*, 8942 – 8943; b) X. Yang, D. Yan, *Adv. Opt. Mater.* **2016**, *4*, 897 – 905; c) Y. Deng, D. Zhao, H. Song, D. Shen, *Chem. Commun.* **2013**, *49*, 5751 – 5753; d) K. Shinichi, K. Takashi, Y. Zhao, O. Hiroyuki, Y. Hideya, *ChemPhotoChem* **2017**, *1*, 102-106; e) S. M. A. Fateminia, Z. Mao, S. Xu, Z. Yang, Z. Chi, B. Liu, *Angew. Chem. Int. Ed.* **2017**, *56*, 12160 – 12164; *Angew. Chem.* **2017**, *129*, 12328 – 12332; f) W. Zhao, Z. He, J. Lam, Q. Peng, H. Ma, Z. Shuai, G. Bai, J. Hao, B. Tang, *Chem* **2016**, *1*, 592 – 602; g) Z. Cheng, H. Shi, H. Ma, L. Bian, Q. Wu, L. Gu, S. Cai, X. Wang, W. Xiong, Z. An, W. Huang, *Angew. Chem. Int. Ed.* **2018**, *57*, 678 – 682; *Angew. Chem.* **2018**, *130*, 686 – 690; h) O. Bolton, K. Lee, H. Kim, K. Y. Lin, J. Kim, *Nat. Chem.* **2011**, *3*, 205 – 210; i) M. S. Kwon, Y. Yu, C. Coburn, A. W. Phillips, K. Chung, A. Shanker, J. Jung, G. Kim, K. Pipe, S. R. Forrest, J. Youk, J. Gierschner, J. Kim, *Nat. Commun.* **2015**, *6*, 8947 – 8956.
[25] a) S. Xu, R. Chen, C. Zheng, W. Huang, *Adv. Mater.* **2016**, *28*, 9920 – 9940; b) S. Hirata, *Adv. Opt. Mater.* **2017**, *5*, 1700116 – 1700166; c) X. Chen, C. Xu, T. Wang, C. Zhou, J. Du, Z. Wang, H. Xu, T. Xie, G. Bi, J. Jiang, X. Zhang, J. N. Demas, C. O. Trindle, Y. Luo, G. Zhang, *Angew. Chem. Int. Ed.* **2016**, *55*, 9872 – 9876; *Angew. Chem.* **2016**, *128*, 10026 – 10030; d) M. Shimizu, T.

Kinoshita, R. Shigitani, Y. Miyake, K. Tajima, *Mater. Chem. Front.* **2018**, *2*, 347 – 354.
[26] K. Nagarajan, G. Gopan, R. T. Cheriya, M. Hariharan, *Chem. Commun.* **2017**, *53*, 7409 – 7411.
[27] T. V. Khuong, J. E. Nuñez, C. E. Godinez, M. A. Garcia-Garibay, *Acc. Chem. Res.* **2006**, *39*, 413 – 422.
[28] K. Baryshnikov, B. Minaev, H. Agren, *Chem. Rev.* **2017**, *117*, 6500 – 6537.

Manuscript received: December 3, 2017
Accepted manuscript online: May 16, 2018
Version of record online: June 10, 2018

